CrossMark

Diffraction-Limited Focusing of Plasmonic Wave by a Parabolic Mirror

P. N. Melentiev [1,2] · A. A. Kuzin [1,3] · D. V. Negrov [3] · V. I. Balykin [1,2]

Abstract
We demonstrate effective, up to 30%, reflection of the surface plasmon-polariton wave (SPP) from a nanogroove made on Ag film surface. The use of SPP reflection from a nanogroove having a shape of parabola helps to realize a new element in nanoplasmonics—parabolic SPP mirror. It was found that the mirror allows focusing of the SPP into a diffraction-limited spot with a lateral size of about λ_{SPP} ($\lambda_{SPP} = 800$ nm—SPP wavelength). The possibility of spatial scanning the focusing spot of SPP on the surface of Ag film is shown.

Keywords Surface plasmon-polaritons · Focusing of SPP · Nanogroove · Parabolic mirror · Ag film

Introduction

Surface plasmon-polaritons (SPP) are surface waves that propagate along the metal-dielectric interface or other metal structures, such as metal films or strips, metal particles of various sizes and shapes, holes in nanofilms, slits, or surface corrugations. SPP waves are nonradiative waves localized along the interface between two media. Choice of a metal for fabrication of SPP elements is crucial in nanoplasmonics. In experimental nanoplasmonics, the noble metals are usually used because of their minimal losses among all known natural materials. Silver, as the main plasmonic material, has minimal losses in the visible and near-infrared regions of the spectrum [1, 2].

A great interest in SPP research is related to the possibility of using SPP as information carriers, because SPP waves combine the advantages of electrons (the possibility of strong spatial localization) and photons (high frequencies) [2–4]. Similar to photon optics, SPP optics describes the excitation, control, and detection of such waves. To date, the following elements of SPP optics are known: mirrors [5, 6], beam splitters [7], waveguides [8, 9], interferometers [10, 11], lenses [12–15], sensors [16–19], and plasmonic nanolasers [20–22].

The elements of SPP optics are fabricated, as a rule, using electron- or ion-beam nanolithography. After the fabrication of such elements, it is no longer possible to change their properties and, which is essential, their mutual arrangement. This feature of SPP optics has both advantages and disadvantages. On the one hand, the high spatial stability of the relative arrangement of SPP elements in space is demanding in applications. On the other hand, the impossibility of changing the mutual arrangement of these elements (as in photon optics) makes it impossible to perform fine-adjustment of the whole optical set up. This, in turn, does not allow reaching the highest characteristics of the SPP optical elements.

Focusing of waves is one of the most important problems of any type of optics (photon optics, atom optics, optics of charged particles), because it allows to couple a plane propagating wave to a spatially localized wave modes. In plasmon optics, waves focusing was realized using the structuring of the surface of a metal film by curved ridges [12], curved slits [15], curved chain of nanoparticles [23], by creating a dielectric lens on the metal film—in a direct analogy with a photon optics [24], or with use of multiple focusing elements [25]. Another important element of the wave focusing is a parabolic mirror. Parabolic mirrors are common elements of photon optics and are notable for the possibility of focusing radiation in a diffraction-limited spot, as well as the absence of chromatic and spherical aberrations. However, in nanoplasmonics, parabolic mirrors have not been realized so far.

✉ P. N. Melentiev
melentiev@isan.troitsk.ru

✉ V. I. Balykin
balykin@isan.troitsk.ru

1   Institute for Spectroscopy Russian Academy of Sciences, Phizicheskaya str., 5, Troitsk, Moscow, Russia 108840

2   Higher School of Economics, National Research University, Moscow, Russia 101000

3   Moscow Institute of Physics and Technology, Moscow Reg., Dolgoprudny, Russia 141700

Springer

In this paper, we demonstrate effective control of SPP wave using a parabolic mirror that allows: (1) reflection of SPP waves with efficiency of up to 30%, (2) focusing of SPP waves into diffraction-limited spot with a lateral size about λ_{SPP}, and (3) spatial scanning the focusing spot of SPP wave on the surface of Ag film.

Optical Media for SPP Waves

The choice of material for creating the SPP optics elements is decisive. Silver and gold are the main materials of modern experimental nanoplasmonics due to their minimal ohmic losses among all known natural materials. It should also be noted the active study of plasmon materials, which can be compatible with silicon microelectronics [1, 26].

Silver, as the main plasmonic material, has minimal losses in the visible and near-infrared spectral regions [1]. In silver nanofilms, there are additional losses due to the corrosion of the metal surface by sulfur and chlorine, which are inevitably present in the environment [27]. An effective approach to prevent corrosion of silver surface is the deposition of thin protective films [28, 29]. A significant number of the nanoplasmonics elements are created on the basis of planar nanofilms. The progress in nanofilms deposition with low losses makes it possible to hope for the possibility of further reduction of losses in metallic nanostructures based on them [30].

The main parameter characterizing the quality of metal nanofilms is the SPP propagation length: the length after which SPP wave intensity decreases to 1/e from its initial value [31]. The SPP propagation length depends strongly on the quality of the nanofilm used, determined by the deposition process. The known values of the SPP propagation length on Ag/air interface are not exceeding 50–80 μm (at a wavelength of 800 nm) [30, 32–34].

In this work, Ag nanofilm was used as an optical medium for SPP waves. As it was recently shown, the use of modern high-vacuum equipment and substrates with low roughness made it possible to create silver films having significantly better plasmonic properties. The SPP propagation length on the surface of Ag films was of the order of 100 μm (at a wavelength of 800 nm) [15]. The measured length of a SPP wave in such a film is considerably larger than in other published works.

In this paper, all measurements were performed in the near-infrared spectral range, at a SPP wavelength of about 800 nm. This wavelength is chosen for several reasons. First, at this wavelength, the losses of Ag nanofilms are significantly smaller in comparison with a visible spectral range. Second, at this wavelength, the sensitive CCD cameras are available, allowing performing optical microscopy of the SPP waves. Third, in this spectral range, the overwhelming majority of works in the field of nanoplasmonics are carried out, which

allows us to compare our results with the results of other laboratories.

SPP Reflection from a Nanogroove

Nanogroove made on the surface of a metal film is one of the basic elements of SPP optics. It is widely used in different applications: (1) to excite SPP waves [35], (2) to detect SPP [15, 36], and (3) to form SPP interferometers [10, 11].

In the paper [5] it was proposed to use a nanogroove made on a surface of nanofilm to reflect SPP waves. The calculations carried out by the authors of this work showed that the reflection coefficient of the SPP from a nanogroove depends on the wavelength of the SPP, the width of the nanogroove, and its depth. The maximum value of the reflection coefficient for the optimally selected parameters was about 30%. For the SPP wavelength considered in this paper, the reflection coefficient of 30% is realized with the following nanogroove parameters: width 100 nm, depth 120 nm [5]. Such parameters were used in the present work to create a parabolic mirror for SPP based on the nanogroove.

Note that the maximum possible reflection of the SPP waves from nanogrooves is several times smaller in comparison with the reflection from the metal nanostrip fabricated on the surface of the metal nanofilm, reaching the reflection values more than 90% [36]. Nevertheless, the simplicity of nanogrooves fabrication, in comparison with the technological difficulties of creating nanostrips, makes it more demanding in that cases when a large value of the reflection coefficient is not required.

Figure 1a shows the optical image of an experimental sample made for measuring the SPP reflection coefficient from a nanogroove. The experimental sample was created from a 200-nm-thick Ag film in which the following structures were made using focused ion beam lithography: (1) an array of nanoholes with a period of 800 nm to excite SPP wave; (2) a "nanogroove-mirror" with a depth of 120 nm and a width of 100, designed to reflect the SPP wave; and (3) two "nanogrooves-detectors," 25 nm deep and 60 nm wide, created to measure the reflected and transmitted through the "nanogroove-mirror" SPP waves by their scattering on these nanogrooves. "Nanogrooves-detectors" are located at equal distances from the "nanogroove-mirror," to measure the ratio of the power of transmitted and reflected SPP waves. The surface of Ag film is covered by nanocaves to visualize the propagation of SPP waves [15]. Nanocaves are located at a distance of 5 μm from each other. The diameter of nanocaves is 60 nm, the depth is 25 nm.

The geometric parameters of the "nanogrooves-detectors" were chosen from considerations of minimal losses for the SPP propagation. Such a regime is realized with nanogroove sizes corresponding to the so-called cut-off mode for the waveguide MDM mode of a nanogroove [37]. With such
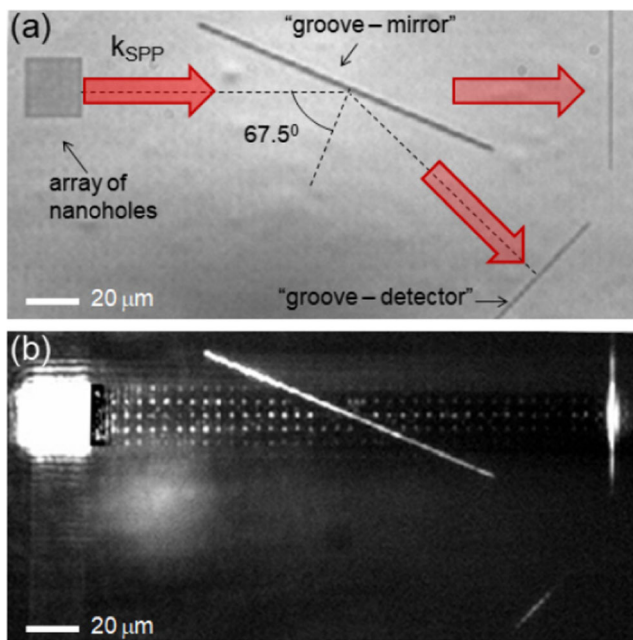
Fig. 1 Experimental realization of SPP reflection from the nanogroove. **a** The image of the experimental sample in an optical microscope when it is illuminated with white light, showing all elements of the sample: the SPP source (array of nanoholes), "nanogroove-mirror," "nanogroove-detectors." **b** The image of the experimental sample in an optical microscope when the array of nanoholes is illuminated by a laser radiation having polarization directed along the rows of the nanoholes array

parameters, a single nanogroove scatters SPP wave with efficiency less than 1% [15].

Figure 1b shows the image of the experimental sample in which excitation, propagation, reflection from a nanogroove, and detection of SPP were studied. The image was obtained with the help of an optical microscope, when the experimental sample was illuminated by a laser radiation with a wavelength of about 800 nm having polarization directed along the rows of the nanoholes array. The laser radiation impinges the sample perpendicular to its surface. Laser radiation illuminates the sample from the side of the quartz substrate and excites SPP waves on the other side of the silver film, adjacent to the air. The diameter of the laser spot corresponds to the size of the matrix with nanoholes and is equal to 20 μm.

The figure shows a bright rectangular spot corresponding to the transmission of light through the array of nanoholes. From the right side of this spot, there are small white spots located in the matrix order. The origin of these spots is the SPP wave scattering on the nanocaves fabricated on the Ag film surface. The scattered radiation on these nanocaves allows us to visualize the propagation of the SPP on the Ag film surface. The transmittance of SPP through the "nanogroove-mirror" element can also be seen from the scattering on the nanocaves. In addition, the figure clearly shows the scattering of SPP on the "nanogroove-mirror." Besides, the reflected and transmitted SPP waves can be seen through the scattering of SPP on

"nanogroove-detectors." The detected signal on the "nanogroove-detector" convincingly demonstrates the mirror reflection of SPP from the "nanogroove-mirror" at an angle of 135^{0}.

From Fig. 1b, it is possible to evaluate the reflection coefficient of SPP from a nanogroove—a ratio of SPP intensity reflected from the nanogroove to the incident SPP intensity. As can be seen from the figure, the most part of SPP wave passes through the "nanogroove-mirror" and only a small part of the SPP wave is reflected. Measurement of the intensity of the SPP wave scattered on the nanocaves before and after the "nanogroove-mirror" on the Fig. 1b helps to obtain the "nanogroove-mirror" transmission of about 91%. The ratio of the scattering intensity of the transmitted and reflected SPP waves on the "nanogrooves-detectors" is approximately equal to 22.7. Thus, the reflection coefficient of the "nanogroove-mirror" is about 4%.

We created a series of samples to measure the reflection of SPP wave at different angles from the nanogroove. The highest reflection coefficient of SPP is realized at normal incidence and is equal to 30%, which corresponds to the calculations carried out in [5]. At the reflection angle of 45%, about 15% of the energy of the SPP is reflected. An increase in the reflection angle leads to a decrease in the reflection coefficient.

SPP Focusing by a Parabolic Mirror

The demonstration of SPP wave reflection from a nanogroove opens up new possibilities to control of SPP waves. In this section, we present experimental demonstration of focusing of SPP wave using a parabolic mirror formed by nanogroove of a specially designed parabolic-type shape fabricated on the surface of a silver film.

Parabolic mirrors are common elements of photon optics and are notable for the possibility of focusing radiation in a diffraction-limited spot, as well as the absence of chromatic and spherical aberrations. In contrast with spherical mirrors, which suffer from a spherical aberration that becomes stronger as the ratio of the beam diameter to the focal distance becomes larger, parabolic mirrors can be made to focus beams of any width. The ideal parabolic surface is not limited in space. In practice, parabolic mirror is only a segment of a parabolic surface. This allows significantly expanding their scope of applications. For example, to get a physical access to the area of focal spot in which the object under investigation can be arranged—a waveguide or other optical elements.

In plasmon optics, the propagation of SPP on flat surfaces is considered; therefore, SPP elements, as a rule, have a two-dimensional topology. In principle, by analogy with photon optics, it is possible to focus SPP wave by its reflection from the parabolic mirror having two-dimensional topology. The wave equations for light and SPP waves are similar, thus the

focusing of the SPP wave should have the same listed above advantages of focusing by a parabolic mirror. In plasmonics, parabolic mirrors were not convincingly realized. Only a few works in this field are known [38, 39].

Let us consider the focusing of SPP wave by a parabolic mirror in two-dimensional coordinates. In this case, the surface of such a mirror will be determined by a two-dimensional curve that has a parabolic dependence on the spatial coordinates in the shape defined by the equation $4Fy = x^2$, where F is the focal length of the parabolic mirror, the coordinates x and y are located in the propagation plane of the SPP wave. In the above equation for a parabola, its vertex is located at the coordinate's origin. The symmetry axis is arranged along the y axis. When the SPP wave propagates with the wave vector $\overrightarrow{k} = \left(0, -\left|\overrightarrow{k}\right|\right)$, the point of focusing of the SPP wave will have the coordinates: $x = 0$, $y = F$.

The scheme for SPP focusing by the parabolic mirror is shown in Fig. 2a. The figure shows the image of the fabricated experimental sample in electron microscope. The sample is formed by 200-nm-thick Ag film, on the surface of which, using ion lithography, the following elements of plasmon optics are created: (1) the array of nanoholes designed for effective excitation of SPP wave [15], (2) a "nanogroove-mirror" having a parabola shape with a focal length of 20 μm, (3) five "nanogrooves-detectors" located in the area of the supposed focusing of the SPP wave, and (4) nanocaves with a diameter of 60 nm and a depth of 25 nm to visualize the propagation of a SPP wave (see [15] for details of nanolithography used). The size of the nanoholes array determines the maximum transverse size of the excited SPP. This size, as well as the focal length of the parabolic SPP mirror, determines the maximum possible SPP wave convergence angle, equal in this case to the value $\theta = 18.5^0$. By analogy with photon optics, this angle determines the diffraction-limited focul spot, equal to $w_0 \approx \frac{2}{k\sin\theta} \approx 810$ nm [40]. In the figure, the arrows show the propagation and focusing of SPP wave.

Figure 2b shows an image of the experimental sample in an optical microscope. The image was obtained with the help of an optical microscope when the array of nanoholes was illuminated by laser radiation at 800 nm and the polarization of the radiation directed along the rows of the matrix with nanoholes. Laser beam is oriented perpendicular to the surface of the sample. The diameter of the laser spot on the sample corresponds to the size of the array with nanoholes and is equal to 20 μm [15]. The figure shows a bright rectangular spot corresponding to the transmission of laser light through the array of nanoholes. To the left of this big bright spot, there are small sports of the equal size that are located in the matrix order. These spots correspond to the scattering signal of the SPP wave on the nanocaves and show the propagation of the SPP wave on the Ag film surface toward the "nanogroove-mirror." The figure also shows the bright curved line that originated from a scattering of the SPP wave on the "nanogroove-mirror." The result of the SPP focusing by the "nanogroove-mirror" is clearly seen by SPP scattering on the "nanogroove-detectors." Indeed, at the place of location of the "nanogroove-detectors" on the Ag film surface, there are aligned spots, showing the position of the caustic of the SPP wave at the very focus of the SPP mirror. The focusing point of the SPP wave corresponds to the position determined by the curvature of the parabolic SPP mirror $4Fy = x^2$, with $F = 20$ μm.

We performed a series of measurements with different experimental samples of parabolic SPP mirrors having different focal lengths of 20, 10, and 5 μm. Figure 3 shows the results of measurements of the lateral intensity distribution of SPP wave in the focal point, measured by SPP scattering on the "nanogroove-detector" (the detector was arranged in the parabolic SPP mirror focal point).

As can be seen from Fig. 3a, with use of parabolic SPP mirror having a 20-μm focal length, it is possible to focus the SPP wave into a spot with 1.1 μm lateral size. A decrease in the focal length of the parabolic SPP mirror to 10 μm leads to a decrease of the lateral size of the SPP in focus to a value about 950 nm (Fig. 3b). A further decrease in the focal length of the parabolic SPP mirror leads to an increase of this size. As can be seen from Fig. 3c, the spot size in this case is about

Fig. 2 SPP parabolic mirror with 20-μm focal length. **a** An image of the experimental sample in an electron microscope. **b** An image of the experimental sample in an optical microscope under illumination the nanohole array by laser radiation
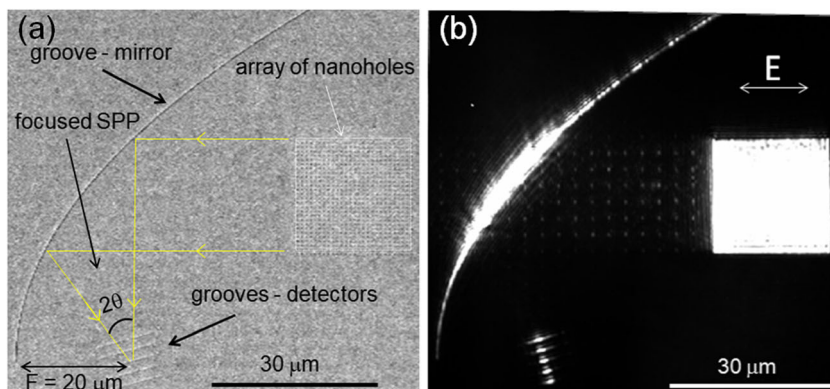
1.25 μm. We attribute this increase to the proximity of the edge of the SPP mirror to the region of SPP focal spot.

The minimal lateral size of SPP wave was realized using focusing with a parabolic SPP mirror having a 10-μm focal length. In this case, the measured lateral size of SPP in focus is about $\delta x_{measured}$= 950 nm. This value is comparable with the value of the diffraction-limited resolution of optical microscope. For the measurement, we used an objective lens having a numerical aperture NA = 0.9. For such an objective, the minimal possible optical resolution is determined by the expression [40]: $\delta x_{min} = 0.6 \frac{\lambda}{NA}$, which is equal to δx_{min}= 530 nm. The physical nature of this limitation is a diffraction of light on the objective lens having limited numerical aperture. Assuming the quadratic contribution of the optical resolution of the microscope objective to the measured value, for the SPP lateral size we will obtain the next expression: $(\delta x_{measured})^2 = (\delta x_{real})^2 + (\delta x_{min})^2$. Under such an assumption it is possible to take into account the numerical aperture of the objective used in the measurements. This gives estimations for a real value of the of SPP lateral size in a focal spot: $\delta x_{real} = \sqrt{(\delta x_{measured})^2 - (\delta x_{min})^2} \approx 800$ nm. Note that this value is about the wavelength of the SPP and corresponds to the diffraction-limited size of the focusing of the SPP wave. Indeed, in this case, the SPP wave convergence angle is $\theta \approx 18.5^0$, and the diffraction limit of the focusing spot is about $w_0 \approx \frac{2}{k \sin \theta} \approx 810$ nm.

One of the important advantages of SPP focusing by parabolic SPP mirror is the ability to control the position of the focal spot on the film surface. This unique feature is due to the dependence of the focal sport position on the incidence angle α of the SPP wave on the parabolic mirror. Thus, to control the spatial position of the focal spot, it is needed to control the angle α of incidence of the SPP wave on the parabolic mirror. In practice, control of the angle α can be performed by changing the incidence angle of the laser radiation on the sample.

At the excitation of a SPP by a nanoholes array, the k vector of the SPP is determined by the following expression [35]:

$$\overrightarrow{k}_{SPP} = \left(\frac{2\pi}{\lambda}\sin\theta\cos\varphi - \frac{2n_x\pi}{\Lambda}\right)\overrightarrow{i}$$
$$+ \left(\frac{2\pi}{\lambda}\sin\theta\sin\varphi - \frac{2n_y\pi}{\Lambda}\right)\overrightarrow{j},$$

here Λ—the period of nanoholes, λ—the wavelength of laser light, n_x, n_y—integers that determine the order of diffraction of laser radiation on the array with nanoholes, θ, and φ are the angles of incidence of the laser beam. The highest excitation efficiency of a SPP wave is realized when one of the diffraction orders n_x, n_y is equal to one, and the other to zero. For example, n_x, = 1, n_y = 0, and the angles of incidence of laser radiation θ and φ are equal to zero (the case of a normal

Fig. 3 Focusing of SPP wave by a parabolic SPP mirrors. The intensity distribution of SPP wave in the focal point for the parabolic SPP mirrors having different focal lengths: (a) F=20 μm, (b) F=10 μm, (a) F= 5 μm
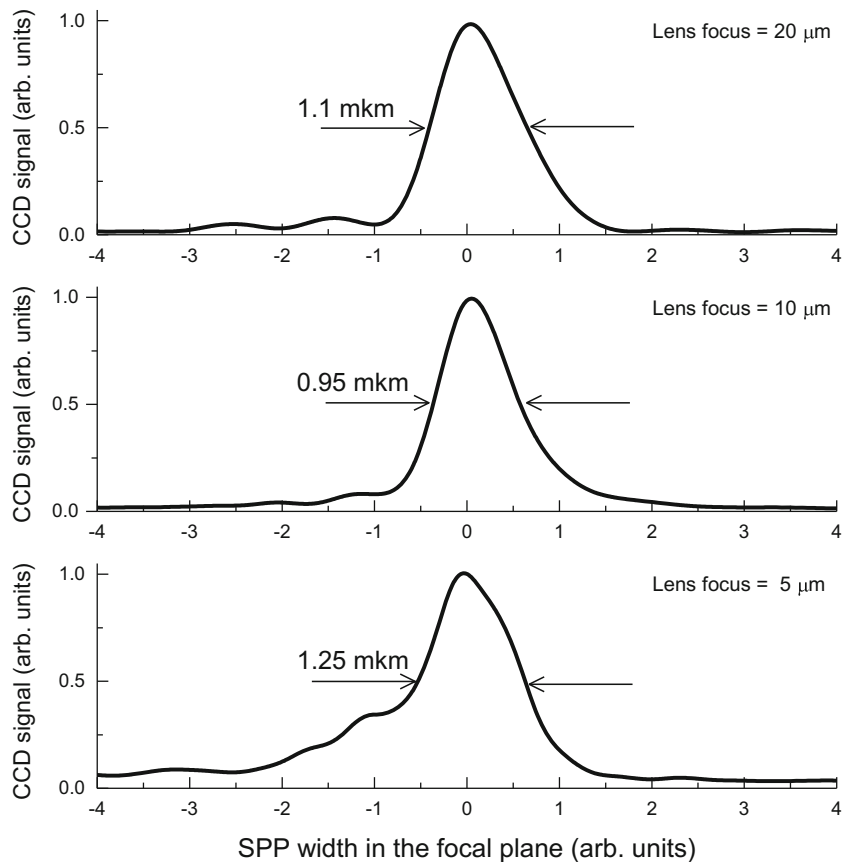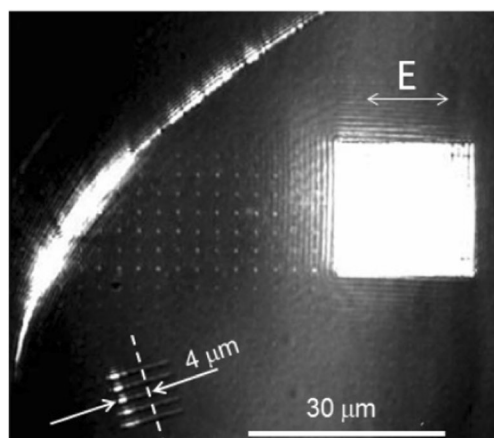
Fig. 4 Control of the focal spot position of SPP wave by a change in the angle of incidence of the laser radiation

incidence of radiation on the sample). In this case, the SPP will propagate along the x axis with a wave vector equal to the reciprocal lattice vector of the array with nanoholes: $\overrightarrow{k}_{SPP} = \left(-\frac{2\pi}{\Lambda}\right) \overrightarrow{i}$. It can be shown that the small tilts of the laser radiation in a plane perpendicular to the x axis (a small non-zero values of the angle θ) will lead to changes in the propagation direction of the plasmon wave. In this case, $\varphi = \pi/2$, and $\sin\theta \approx \theta$. Thus, the k vector of the SPP is $\overrightarrow{k}_{SPP} = \left(-\frac{2\pi}{\Lambda}\right) \overrightarrow{i} + \left(\frac{2\pi}{\Lambda}\theta\right) \overrightarrow{j}$, i.e., small deviations of the angle θ from its zero value, leads to the appearance of a small value of the transverse component of the SPP k vector, and the SPP propagates at a small angle $\alpha \approx (\Lambda/\lambda)\theta$ to the x axis.

Figure 4 shows the possibility of controlling position of the focusing spot of the SPP wave by a parabolic mirror. The focal length of parabolic SPP mirror is equals to 20 μm. The image was obtained with the use of a weak illumination of the experimental sample with white light, which allows to see not only the point of focusing of the SPP wave, but also the location of the "nanogrooves-detectors." The figure demonstrates that the point of focusing of the SPP wave can be shifted up to 4 μm from the central position marked in the figure with a dashed line (see also Fig. 3b). The ability to control the point of focusing of the SPP wave is important for different applications of nanoplasmonics. In particular, this approach can be used to couple the SPP waveguides.

Conclusion

In this paper, we have studied the reflection of SPP waves by nanogroove made on the Ag film surface. It is shown that the reflection coefficient of SPP wave can reach a value as high as 30%.

A "nanogroove-mirror" having a parabola shape and a high value of the SPP propagation length on Ag film surface (~100 μm) made it possible to focus the SPP wave to a diffraction-limited spot. The possibility of scanning the point of focusing of SPP wave on the surface is shown. The demonstrated approach to control SPP waves opens the possibility of creating complex optical circuits using SPP waves in all-optical devices based on the use of surface plasmon-polaritons.

References

1. West PR (2010) Searching for better plasmonic materials. Laser Photon Rev 4:795
2. Balykin VI, Melentiev PN (2018) Optics and spectroscopy of individual plasmonic nanostructure. Physics-Uspekhi 61. https://doi.org/10.3367/UFNe.2017.06.038163
3. Brongersma ML, Shalaev VM (2010) The Case for Plasmonics. Science 328:440–441
4. Zia R, Schuller JA, Chandran A, Brongersma ML (2006) Plasmonics: the next chip-scale technology. Mater Today 9:20–27
5. Kuttge M, García de Abajo FJ, Polman A (2009) How grooves reflect and confine surface plasmon polaritons. Opt Express 17:10385
6. Oulton RF, Pile DFP, Liu Y, Zhang X (2007) Scattering of surface plasmon polaritons at abrupt surface interfaces: Implications for nanoscale cavities. Phys Rev B 76:035408
7. Ditlbacher H, Krenn JR, Schider G, Leitner A, Aussenegg FR (2002) Two-dimensional optics with surface plasmon polaritons. Appl Phys Lett 81:1762–1764
8. Krasavin AV, Zayats AV (2007) Passive photonic elements based on dielectric-loaded surface plasmon polariton waveguides. Appl Phys Lett 90:211101
9. Melentiev PN, Kuzin AA, Balykin VI, Ignatov AI, Merzlikin AM (2017) Dielectric-loaded plasmonic waveguide in the visible spectral range. Laser Phys Lett 14:126201
10. Temnov VV, Nelson KA, Armelles G, Cebollada A, Thomay T, Leitenstorfer A, Bratschitsch R (2009) Femtosecond surface plasmon interferometry. Opt Express 17:8423
11. Melentiev PN, Kuzin AA, Gritchenko AS, Kalmykov AS, Balykin VI (2017) Femtosecond plasmon interferometer. Opt Commun 382:509–513
12. Radko IP, Bozhevolnyi SI, Brucoli G, Martín-Moreno L, García-Vidal FJ, Boltasseva A (2009) Efficient unidirectional ridge excitation of surface plasmons. Opt Express 17:7228
13. Volkov VS, Bozhevolnyi SI, Rodrigo SG, Martin-Moren L, García-Vidal FJ, Devaux E, Ebbesen TW (2009) Nanofocusing with Channel Plasmon Polaritons. Nano Lett 9:1278–1282
14. Dennis Brian S et al (2015) Diffraction limited focusing and routing of gap plasmons by a metal-dielectric-metal lens. Opt Express 23:21899–21908
15. Melentiev PN, Kuzin AA, Balykin VI (2017) Control of SPP propagation and focusing through scattering from nanostructures. Quant Electron 47:266–271

16. Homola J, Sinclair SY, Gauglitz G (1999) Surface plasmon resonance sensors: review. Sensors Actuators B Chem 54:3–15

17. Min BK, Kim SJ, Kim D (2007) Appl Opt 46:5703

18. Tong L, Wei H, Zhang S, Xu H (2014) Recent Advances in Plasmonic Sensors. Sensors 14:7959–7973

19. Melentiev P, Kalmykov A, Gritchenko A, Afanasiev A, Balykin V, Baburin A, Ryzhova E, Filippov I, Rodionov I, Nechepurenko I, Dorofeenko A, Ryzhikov I, Vinogradov A, Zyablovsky A, Andrianov E, Lisyansky AA (2017) Plasmonic nanolaser for intracavity spectroscopy and sensorics. Appl Phys Lett 111:213104

20. Bergman DJ, Stockman MI (2003) Surface plasmon amplification by stimulated emission of radiation: quantum generation of coherent surface plasmons in nanosystems. Phys Rev Lett 90:027402

21. Stockman MI (2008) Spasers explained. Nat Photon 2:327–329

22. Noginov MA, Zhu G, Belgrave AM, Bakker R, Shalaev VM, Narimanov EE, Stout S, Herz E, Suteewong T, Wiesner U (2009) Demonstration of a spaser-based nanolaser. Nature 460:1110–1112

23. Evlyukhin AB, Bozhevolnyi SI, Stepanov AL, Kiyan R, Reinhardt C, Passinger S, Chichkov BN (2007) Focusing and directing of surface plasmon polaritons by curved chains of nanoparticles. Opt Express 15:16667–16680

24. Kim H, Hahn J, Lee B (2008) Focusing properties of surface plasmon polariton floating dielectric lenses. Opt Express 16:3049–3057

25. Zhao C, Liu Y, Zhao Y, Fang N, Huang TJ (2013) Nat Commun 4: 2305

26. Boltasseva A, Atwater HA (2011) Low-loss plasmonic metamaterials. Science 331:290–291

27. Graedel TE (1992) Corrosion mechanisms for silver exposed to the atmosphere. J Electrochem Soc 139:1963

28. Zhang XY et al (2006) Ultrastable substrates for surface-enhanced raman Spectroscopy: Al2O3 overlayers fabricated by atomic layer deposition yield improved anthrax biomarker detection. J Am Chem Soc 128:10304–10309

29. Im H, Lindquist NC, Lesuffleur A, Oh SH (2010) Atomic layer deposition of dielectric overlayers for enhancing the optical properties and chemical stability of plasmonic nanoholes. ACS Nano 4: 947–954

30. Wu Y, Zhang C, Estakhri NM, Zhao Y, Kim J, Zhang M, Liu XX, Pribil GK, Alù A, Shih CK, Li X (2014) Intrinsic optical properties and enhanced plasmonic response of epitaxial silver. Adv Mater 26: 6106–6110

31. Raether H (1988) Surface plasmons on smooth surfaces. Springer, Berlin Heidelberg

32. Dawson P, de Fornel F, Goudonnet JP (1994) Imaging of surface plasmon propagation and edge interaction using a photon scanning tunneling microscope. Phys Rev Lett 72:2927–2930

33. Hong HY, Ha JS, Lee SS, Park JH (2017) Effective propagation of surface Plasmon Polaritons on graphene-protected single-crystalline silver films. ACS Appl Mater Interfaces 9:5014–5022

34. Park JH, Ambwani P, Manno M, Lindquist NC, Nagpal P, Oh SH, Leighton C, Norris DJ (2012) Single-crystalline silver films for Plasmonics. Adv Mat 24:3988–3992

35. Maier SA (2007) Plasmonics: fundamentals and applications. Springer Science & Business Media, New York

36. Kress SJP, Antolines FV, Richner P, Jayanti SV, Kim D, Prince F, Ridinger A, Fisher MPS, Mayer S, McPack KM, Pulikakos D, Norris DJ (2015) Nano Light 15:6267–6275

37. Liu JSQ, White JS, Fan S, Brongersma ML (2009) Side-coupled cavity model for surface plasmon-polariton transmission across a groove. Opt Express 17:17837–17848

38. Bozhevolnyi S, Boltasseva A et al (2007) Opt Express 15:6576

39. Smolyaninov II, Hung Y-J, Davis CC (2005) Surface plasmon dielectric waveguides. Appl Phys Lett 87:241106

40. Novotny L, Hecht B (2012) Principles of nano-optics. Cambridge university press, Cambridge